13 NMR in Correlated Electron Systems: Illustration on the Cuprates

Henri Alloul
Laboratoire de Physique des Solides - CNRS
Université Paris-Sud and Université Paris-Saclay

Contents

E. Pavarini, E. Koch, J. van den Brink, and G. Sawatzky (eds.)
Quantum Materials: Experiments and Theory
Modeling and Simulation Vol. 6
Forschungszentrum Jülich, 2016, ISBN 978-3-95806-159-0
http://www.cond-mat.de/events/correl16

1 Introduction: NMR basics

The electronic properties of solids were, in the first half of the twentieth century, considered mostly in the framework of an independent electron approximation with spin degeneracy. Their resulting electronic band structure is such that each electronic level could be doubly occupied. In such an approach one expects metals or insulators with no significant magnetic properties [1]. The traditional experimental studies of the electronic states in such solids usually require a determination of their electronic band structure and an investigation of its effects on the physical properties. Those are usually experimentally obtained by measurements taken at the macroscopic scale such as optical, transport, and magnetic data. To go beyond these approaches Nuclear Magnetic Resonance is thoroughly used. This technique, discovered in the mid of the 20th century is essential as it permits to perform atomic-scale measurements in the materials, differentiating the properties which can be attributed to specific phases or sites in the structure. The aim of this lecture is to present the main physical parameters accessible to NMR experiments, and to illustrate how they do reflect many aspects which are specific to the occurrence of electronic correlations in materials.

Correlations are at the origin of many exotic electronic properties of a series of compounds which have emerged from recent experimental observations. The most important phenomena discovered are related with electronic magnetic properties, which have been quite accessible to Nuclear Magnetic Resonance techniques. They specifically permit to distinguish the orbitals or electronic bands responsible for magnetism, metallic, and superconducting behaviors. They revealed quite often the physical properties which are distinct what is expected within an independent electron scheme.

In non-interacting electronic systems, one considers energy levels with spin degeneracy and fills them with two electrons per level, without any consideration of U, the local Coulomb repulsion on the atomic orbitals. But, as soon as one considers a solid which displays magnetic properties, the latter has to be considered, as U is responsible for atomic and solid-state magnetism. This is fully described in various other lectures in the present series of books.

If one starts with a completely free electron gas, the first incidence of weak correlations can be expressed in a Fermi liquid approach, that is, the electronic states at the Fermi level are not single-particle but rather quasiparticle states in which the electron is dressed by an electronic cloud which involves the electronic correlations. Those quasiparticles are populated in a same way as free-electron states, except that the population jump at the Fermi level is smaller than unity. Correspondingly these quasiparticles have effective masses $m^\star$ which differ from the electron mass. This is seen for instance in the magnitude of the specific heat and the Pauli-like spin susceptibility.

With increasing electron correlations one reaches situations where electron states are in an intermediate regime between independent extended electronic states and local states. Those intermediate electronic states are at the basis of the correlated electron physics which gives exotic properties to the materials and various competing low T states which are often far from being understood at this time.

As the NMR technique is described at length in various books and articles (see Wikipedia and Scholarpedia) for its applications in chemistry, biology, and medical sciences, we shall only recall very briefly the technical principles of NMR in the next section. However we shall recall in more detail the couplings between nuclear spins and electron spins in section 1.2. Those are essential to allow one to probe by NMR the electronic and magnetic properties of solids.

1.1 The magnetic resonance phenomenon: basic applications

Let us recall that the physical properties of solids, and in particular their magnetic properties, are of course determined by the electronic states. On the other hand, the nuclear spin moments, which do not affect these properties, provide an extremely useful probe for the electronic properties. Atomic nuclei are made up of neutrons and protons, which are spin 1/2 particles. They are assembled into quantum states in which the nuclear ground state has a total spin $\boldsymbol{I}$ that may be integer or half-integer. The associated magnetic moment $\boldsymbol{\mu}_{\rm n}$ is proportional to the magnetic moment of the proton $\mu_{\rm p}$, where the multiplicative factor is analogous to the Landé factor for an atomic electronic moment. Each atomic nucleus thus has a specific magnetic moment $\boldsymbol{\mu}_{\rm n} = \hbar\gamma_{\rm n}\boldsymbol{I}$. The gyromagnetic ratio $\gamma_{\rm n}$ is known to great accuracy for each of the stable isotopes in the periodic table. Since $\mu_{\rm p} \simeq 10^{-3}\mu_{\rm B}$, the nuclear moments are extremely small, as are their mutual interactions. As a consequence, they are almost always in a paramagnetic state with a Curie magnetization $\mu_z = N(\hbar\gamma_{\rm n})^2 I(I+1)B_0/3k_BT$. We see immediately that, in a given applied field, the nuclear magnetization is about 10^6 times smaller than the electronic magnetization. The nuclear magnetism is practically impossible to detect using just macroscopic magnetization measurements taken on bulk samples. But, although the nuclear magnetic susceptibilities are weak, they can be detected by magnetic resonance which is a spectroscopy that permits a selective detection of the nuclear spin response.

Discovered at the outset of the second world war by F. Bloch and E.M. Purcell, the nuclear magnetic resonance technique has rapidly become a unique method to investigate the chemical and physical properties of condensed matter [2, 3]. Its success results from the fact that it resolves spectroscopically the properties of the nuclear spins of the distinct atomic species present in a material. A homogeneous applied external magnetic field B_0 induces a splitting of the nuclear-spin energy level $h\nu_L = \hbar\gamma_{\rm n}B_0$ which usually falls in the radio-frequency range of the order of 10 MHz per Tesla. The absorption of a radio-frequency field at the adequate frequency ν_L permits to detect the presence of the corresponding nuclei.

One highlight of NMR is the acquired possibility to provide images of the spatial distribution of ^{1}H nuclei in-vivo in biological matter, which is the basis of medical Magnetic Resonance Imaging (MRI). Though this is the most popular application of NMR known by a large audience, NMR is an even more powerful technique when one uses the interactions of given nuclear spins in a material with their neighboring atomic states. This results in rich spectroscopic splittings of the NMR lines, which permit to locate the atoms in molecular states and therefore to determine the molecular structures in chemistry or in the solid state. Such spectroscopic techniques have been revealed since the 1960s but their impact has been tremendously highlighted by the

improvement of the superconducting-magnet industry which has allowed to produce extremely homogeneous magnetic fields B_0 as large as 21 Tesla with negligible drift in time. In the corresponding range of frequencies ν_L, exceptionally stable coherent sources are available, with narrower spectral widths than the transitions to be observed. These are obtained by electronic oscillators with frequency stabilized on the resonant mode of a piezoelectric quartz crystal. Moreover, for such frequencies, very powerful amplifiers are also available. High intensity radio-frequency pulses are used to significantly modify the populations of the spin quantum states. This approach is essential for nuclear spin relaxation studies. Therefore on the electronics side, NMR has highly benefited from all the developments of the fast semiconductor and computing capabilities associated with the expansion of information technologies.

1.2 Electronic hyperfine couplings

It is clear that changes in the magnetic induction in a material can be detected directly by a change in the nuclear Larmor frequency. In weakly magnetic materials, for which the magnetization is negligible, $B_0 = \mu_0 H_a$ and the nuclear Larmor frequency ν_L should be determined solely by the applied external field H_a. It would be difficult to obtain information about the physical properties of materials in such a limit. But we have to recall that the nucleus is a kind of atomic scale microscopic probe, coupled to the electrons. Interactions like the dipole interactions between nuclear and electronic spins are such that the nuclear spin feels a magnetic field associated with the polarization of the electronic magnetic moments. This means that the magnetic field felt by the nuclear spins is modified with respect to the applied field. It is the spectroscopy of these fields that provides atomic scale information about the immediate vicinity of the nuclei in the material. Let us examine the different on-site interactions between the nuclear spins and the magnetic moments of electronic origins, known collectively as hyperfine interactions [2, 3].

The dipole interaction between the moments associated with a nuclear spin $\boldsymbol{I}$ and an electron spin $\boldsymbol{S}$ separated by a displacement $\boldsymbol{r}$ is

$$H_{dd} = -\frac{\mu_0}{4\pi}\frac{\gamma_e\gamma_n\,\hbar^2}{r^3}\left[\boldsymbol{I}\cdot\boldsymbol{S} - \frac{3(\boldsymbol{I}\cdot\boldsymbol{r})(\boldsymbol{S}\cdot\boldsymbol{r})}{r^2}\right], \tag{1}$$

where γ_n and γ_e are the nuclear and electronic gyromagnetic moments, respectively, and $\boldsymbol{S}$ and $\boldsymbol{I}$ are here dimensionless quantities. This dipole interaction diverges when r tends to zero, and is therefore only valid for electrons with zero probability of being at the site of the nucleus. This is the case for electrons in the p, d, or f shells. On the other hand, the s electrons have nonzero probability of being at the site of the nucleus. The Dirac Hamiltonian can be used to show that the corresponding interaction, called the contact interaction H_c is scalar, and is given in this case by

$$H_c = \frac{\mu_0}{4\pi}\frac{8\pi}{3}\,\gamma_e\gamma_n\,\hbar^2\;\;\boldsymbol{I}\cdot\boldsymbol{S}\,\delta(\boldsymbol{r})\,. \tag{2}$$

Finally, the interaction with the magnetic field associated with the orbital angular momentum

of the electron is

$$H_{\rm orb} = -\frac{\mu_0}{4\pi}\gamma_e\gamma_n\,\hbar^2\;\frac{\boldsymbol{I}\cdot\boldsymbol{\ell}}{r^3}. \tag{3}$$

These Hamiltonians can all be written in the form

$$H_{\rm eff} = -\gamma_n\,\hbar\,\boldsymbol{I}\cdot\boldsymbol{B}_{\rm eff} \tag{4}$$

and we may consider that each electron induces a magnetic field $\boldsymbol{B}_{\rm eff}$ at the nuclear site. As the temporal fluctuations of the electronic moments are very fast compared with the nuclear Larmor frequency, the static component of $\boldsymbol{B}_{\rm eff}$ is its time average. The position of the NMR for a given nucleus is thus determined by the time average $\boldsymbol{B}_{\rm eff}$ of the resultant of the fields due to the different electrons in the material. It is easy to see that the hyperfine interaction will vanish for filled electronic shells, because they have zero total spin and total orbital angular momentum. When there is no applied field, $\boldsymbol{B}_{\rm eff}$ can only be nonzero for materials in which there is a static spin or orbital magnetic moment. This will be the case for magnetically ordered materials. The weakness of the interaction between electronic and nuclear spins permits to consider the nuclear spins as somewhat ideal probes of the electronic properties of materials. Those are essentially obtained from measurements of the NMR shifts or spin-lattice relaxation parameters that we shall describe in some details in these lecture notes, which are organized as follows:
It will be shown first (section 2) that in metals the Pauli paramagnetism, that is the electronic density of states is accessible through NMR-shift data. Then, in section 3, we shall demonstrate that NMR spectra do give clear evidence of the local effects induced by impurities. Such experiments permit as well (Sec. 3.1) to understand that the nuclear spins are not limited to the detection of on-site magnetic responses, but do sample as well the behavior of nearby sites through transferred hyperfine couplings.
The good knowledge of the NMR characteristics in solids for which non-interacting electron theories apply quite well, naturally permitted in the initial experiments on correlated electron systems to detect the unexpected modifications of electronic properties that occurred in such materials. This appears as an advantage of the NMR technique, with respect to most recent experimental probes which have been developed specifically to study strongly correlated electron systems. This will be illustrated in section (section 4) on two cases highlighted by NMR-shift data on important correlated physics cases. First in Sec. 4.1, we discuss the relatively simple case of the NMR studies on the magnetic properties of $3d$ impurities in metallic sp metals, well known as the "Kondo effect". This has been the earliest correlated-electron physics case which has been understood. It has opened the way to the studies of heavy fermions and Kondo lattices which are touched on in Ref. [4]. The second case is that of the high-T_c cuprates, which is of course the family of compounds that has attracted a large interest on correlated-electron physics. NMR hyperfine-coupling studies in the cuprates permitted to understand the actual electronic structure. Furthermore the NMR-shift data in the low doping part of the phase diagram were the first experimental evidence for the occurrence of a pseudogap as will be detailed in Sec. 4.3. NMR spectra taken on cuprates with substituted impurities permitted as well to reveal the magnetic properties of the pure correlated electron system, as detailed in Sec. 4.4.

Other important parameters accessible to NMR experiments are the longitudinal and transverse nuclear spin-lattice relaxations. Those processes will be recalled in section 5. They quite generally permit to use the dynamics of the nuclear magnetization to probe the excited electronic states in condensed matter. In correlated electron systems the comparison with NMR-shift data using eventually data taken on different sites of the atomic structure do give important indications on the strength of the electronic correlations (Sec. 5.3). Such measurements give access to determinations of electronic gaps in some electronic structures.
Such gaps are important in the case of superconductors as they do reflect the pairing of electrons in the superconducting state. Their existence can be probed by the large incidence on NMR-shift and spin-lattice relaxation NMR data (Sec. 6). The study of exotic superconductivities and the capability of NMR to give some hints on the symmetry of the superconducting order-parameter are illustrated in Sec. 6.3.

2 NMR shifts

In a material, each of the distinct hyperfine couplings listed above induces a specific contribution to the NMR shift. Those are of course quite dependent on the magnitude of the corresponding hyperfine coupling and of the electronic state of the considered material.

2.1 Chemical shifts

In substances where the electrons are paired in atomic or molecular orbitals, the static part of the hyperfine coupling is only nonzero in the presence of an applied field $\boldsymbol{B}_0$, and is proportional to $\boldsymbol{B}_0$ as is the magnetization. The resonance is shifted with respect to that of the free atom in a gas. The relative shift $\boldsymbol{B}_{\rm eff}/\boldsymbol{B}_0$ may be due to the orbital part of the hyperfine coupling. This is the case, for example, for the displacement due to the orbital currents induced by the external magnetic field in electronic or molecular shells close to the nucleus. Since this shift depends on the electronic charge distributions, it is highly sensitive to the chemical environment of the given atom, hence the name chemical shift. These effects are generally small, and expressed in parts per million (ppm) but can be used to distinguish the nuclear spin resonances of the different atoms depending on their environment. This has become a very powerful tool, used universally in chemistry and biology. Routine chemical analyses are carried out by NMR. It also helps one to determine the 3D structures of biological molecules, using multidimensional methods, which have reached an exceedingly high level of refinement.

2.2 Knight shifts in metals

When the electron states are not paired in molecular states or in bonds, the spin degeneracy of the electronic states might be lifted by the applied field, as for electron states at the Fermi level in a metallic band. In that case a $\boldsymbol{B}_{\rm eff}$ component due to the electronic atomic moment may arise via the contact hyperfine term. In a metal the corresponding frequency shift K of the Larmor

frequency is called Knight shift [5] and is directly proportional to the Pauli spin susceptibility χ_{P0} of the metallic band. In usual metallic systems such as alkali metals the early-day studies by NMR permitted to demonstrate that this technique gives indeed the best evaluation of the electronic spin susceptibility. Assuming that the main hyperfine coupling is the direct on-site contact interaction of Eq. (2), which can be written $H_c = A_0\ \boldsymbol{I} \cdot \boldsymbol{S}\ \delta(\boldsymbol{r})$ this yields an NMR Knight shift

$$K = A_0 \chi_{P0} / (g \mu_B \hbar \gamma_{\rm n})\,. \tag{5}$$

In such simple metals the spin susceptibility $\chi_{P0} = (g\mu_B)^2 \rho(E_F)/2$ measures the actual density of states $\rho(E_F)$ taken per spin direction at the Fermi level, which is typically T-independent as the conduction-electron bandwidth is usually quite large and the Fermi level much higher than $k_B T$. The Knight shift is usually a large quantity which is measured in %. This comes about because the contact coupling A_0 is usually much larger than the corresponding dipole or orbital couplings, which permits to sense very effectively the Pauli susceptibility.

2.3 NMR in magnetic materials

In magnetic materials, the electronic moments are static at low temperatures, as compared with their behavior at the Curie or Néel temperatures. It follows that the static effective fields are nonzero even in the absence of any applied field. For atomic nuclei carrying an electronic moment, this field will be very large (several Tesla in general), and will give rise to a resonance at the Larmor frequency $h\nu_L = \hbar \gamma_{\rm n} B_{\rm eff}$, which can be detected in the absence of an applied external field. One speaks then of Zero Field Nuclear Magnetic Resonance (ZFNMR). The fields induced on the nuclear spins of non magnetic atomic sites are generally weaker but can still give valuable information on the properties of the magnetic state.

3 Impurities: example of transferred hyperfine couplings

All real crystalline materials contain structural defects. Those are often impurity atoms substituting some atoms in the ideal structure, or disorder induced by vacancies on some sites of the atomic structure or by deviations to the ideal structural arrangement of atoms. The incidence of specific substituted impurities on the physical properties of the material is sometimes well understood. The essence of the observed phenomena is that an impurity is a local screened Coulomb potential, which ideally is a uniform perturbation in $\boldsymbol{q}$ space inducing a response, which is inhomogeneous in real space but which reflects the response to all $\boldsymbol{q}$ values. In a classical metallic system, since the response is homogeneous up to $|\boldsymbol{q}| = k_F$, the main detected feature comes from this truncation of the response at k_F, which yields the well known Friedel oscillations in the local density of states for a charge defect, and the RKKY oscillation for a spin defect. Such effects differentiate the electronic response on sites in the vicinity of the defect and can be detected by NMR experiments. We shall first illustrate this in the case of magnetic defects in sp metals and show that NMR spectra permit to probe directly the RKKY oscillations.

3.1 Local RKKY spin-density oscillations induced by magnetic impurities in metals

If one substitutes a magnetic impurity on a lattice site of a metal such as Cu, the neighboring sites are differentiated and the magnetic response depends on the distance to the impurity. For local moment impurities, Yosida [6] calculated explicitly the spin-density oscillations assuming that the free electron spin s and local moment S interact by an exchange interaction

$$H = -J\ \boldsymbol{S}\cdot\boldsymbol{s}\ \delta(\boldsymbol{r}). \tag{6}$$

The resulting local spin density, calculated in perturbation theory at a position R_n with respect to the impurity is given by

$$n(R_n) = -\frac{1}{4\pi} J\rho(E_F)\ \frac{\cos(2k_F R_n)}{R_n^3}\ \langle S_z\rangle \tag{7}$$

for a field applied in the z direction. For local-moment impurities such as Mn in Cu the NMR Knight shift of a Cu nuclear spin at position R_n with respect to the impurity acquires an extra shift ΔK given in an applied field H by

$$H\Delta K(R_n) = A_{\rm hf}\ n(R_n) = A(R_n)\langle S_z\rangle, \tag{8}$$

where $A_{\rm hf}$ is the on-site Cu hyperfine coupling. In most dilute alloys of transition elements only a few near-neighbor shells of the impurity could be resolved. However in Cu-Mn, the impurity magnetization $\langle S_z\rangle$ becomes so large at low T and high fields that $n(R_n)$ becomes sizable on many neighboring sites of the impurity. Up to 17 distinct shells of neighbors could be detected in that case, as can be seen in the spectra of Fig. 1, which gives a straightforward illustration of the occurrence of spin-density oscillations. One can see that there are about as many extra lines (we call them satellite lines) on the right and on the left of the central line. The technical details about the assignment of the different lines to specific shells of neighbors, and the analysis of the spatial dependence of the spin polarization which can be deduced from those data are summarized in Ref. [7]. One could push the analysis to a stage permitting to confirm the overall R_n^{-3} dependence, but also to evidence deviations from the asymptotic limit at short distances. Such deviations with respect to the spatial dependence of Eq. (7) could be analyzed by using a more reliable model than an exchange coupling between the impurity and electron spins.

3.2 Transferred hyperfine couplings

So far we have only considered hyperfine couplings between nuclear spins and the electrons involved in the atomic orbitals of the corresponding site. However the above illustration of the RKKY interaction did allow us to demonstrate that electrons on a given atomic site interact as well with the neighboring sites. Indeed, if we consider Eq. (8) we see that it permits to define a transferred hyperfine coupling $A(R_n)$ between the local moment at the origin and the nuclear spin at R_n.

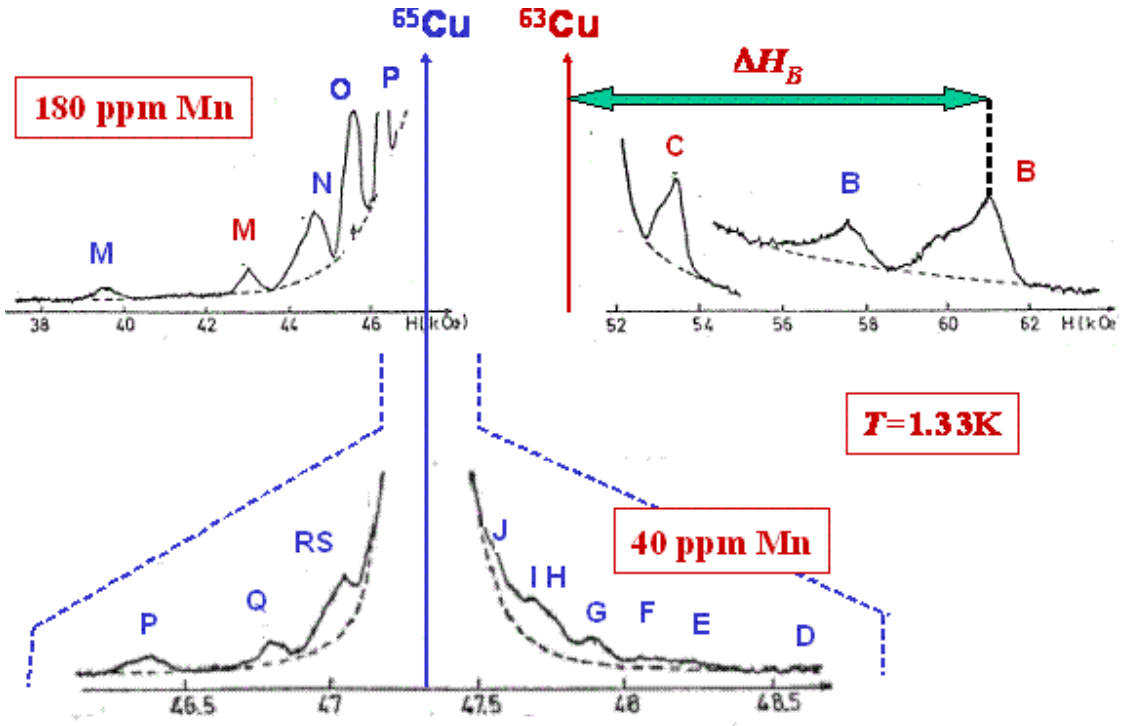

Fig. 1: *NMR spectra of the ^{63}Cu and ^{65}Cu nuclear spins in dilute Cu-Mn alloys obtained by sweeping the applied external field, at 1.3 K. The spectra have been expanded vertically to exhibit the satellite lines by cutting the large intensity central lines at the pure copper NMR positions, which are pointed by arrows. On both sides of the central lines one can see the weak NMR signals of the diverse copper shells of neighbors. The sites far from the impurities are better resolved by reducing the impurity concentration, as shown in the expanded bottom spectrum. (adapted from Ref. [7])*

Therefore, in systems where different atomic sites with distinct electronic properties are involved in a unit cell, such transferred hyperfine couplings do play an important role. In particular, if one considers atomic sites which are not displaying the most important magnetic response they will still sense the response of the magnetic sites through such transferred hyperfine couplings. In the case of Cu-Mn the transferred hyperfine coupling with the Mn magnetism extends over a large number of Cu sites. But, as the transferred hyperfine coupling decreases strongly with distance, it is often sufficient to consider solely transferred hyperfine couplings with the first nearest neighbors. For instance in a square lattice such as that of the CuO_2 planes of cuprate superconductors, for which the electronic magnetic response is located on the Cu sites, the ^{63}Cu nuclei will be coupled to the on-site magnetic response and with that of the near neighbors. This can be cast in a combined wave-vector $\boldsymbol{q}$-dependence of the hyperfine coupling $A(\boldsymbol{q}) = A_0 + \sum A_i \, e^{i\boldsymbol{q}\cdot\boldsymbol{r}_i}$ in which A_0 is the on-site local hyperfine interaction between the observed nuclear and electron spins and A_i is the hyperfine interaction with electron spins at neighboring sites at $\boldsymbol{r}_i$. We shall see later that these transferred hyperfine couplings are important for the nuclear spin-lattice relaxation induced on the various atomic sites of the structure.

4 Correlation effects: some incidences on hyperfine couplings and NMR shifts

In this section we shall consider how correlation effects can influence the electronic structure and spin susceptibilities. One of the initially most studied cases is that of the Kondo effect, which was expected to induce a modification of the spin susceptibility of a Kondo impurity and of the induced spin polarization in the host metal. Another important effect is the pseudogap which appears in the underdoped cuprates and has been discovered by NMR-shift experiments.

4.1 Magnetic impurities and Kondo effect

One of the first correlated-electron physics problem which has been fully solved has been revealed by studies of $3d$ impurities substituted on the atomic sites of regular sp metals. One usually assumed that a local moment S resides on the $3d$ sites and interacts with the free electron spin s by the exchange interaction of Eq. (6).

The Kondo problem arose with the discovery by J. Kondo that perturbation theory of the Hamiltonian of Eq. (6) resulted in a $-\ln T$ term in the resistivity of the alloys, which was indeed observed experimentally. It was understood that the conduction-electron interaction with the local moment induced a crossover of the impurity electronic state towards a low-T ground state quite different from the quasi-free local moment and that the crossover temperature defines an energy scale

$$k_B T_K = E_F \, \exp\left[\frac{1}{J\,\rho(E_F)}\right]. \tag{9}$$

This expression for the Kondo temperature T_K bears some analogy with that of T_c and the energy-gap variation with electron-phonon coupling for superconductivity. It has been harder to qualify the actual properties of the Kondo ground state, but from the observed transport and thermodynamic properties associated with the impurity degrees of freedom, it has been accepted rather soon that the impurity properties experimentally appear to evolve from a high-T magnetic state to a non-magnetic like behavior below T_K. In other words, the weak coupling regime where the impurity moment can be treated in a perturbation scheme evolves at low-T into a strong coupling regime, where the impurity and conduction electrons are bound into the ground state. The basic picture which was initially accepted is that the conduction electrons might form a singlet state with the impurity and compensate its magnetization. If such a spatially extended state occurs, one would expect to see its experimental signature on local magnetic measurements in the corresponding spatial range around the impurity, so that NMR experiments appeared as the ideal probe to view such effects. From the study of the macroscopic properties of impurities in noble metal hosts, it was established that the crossover temperature T_K was highly dependent on the impurity. This was, of course, quite compatible with the exponential expression of Eq. (9). Values of T_K could be estimated from the maximum in the impurity contribution to the specific heat or from the Weiss contribution to the spin susceptibility measured at high enough temperature, etc. This permitted to establish that T_K was below 10 mK for Cu-Mn, ~ 1 K for

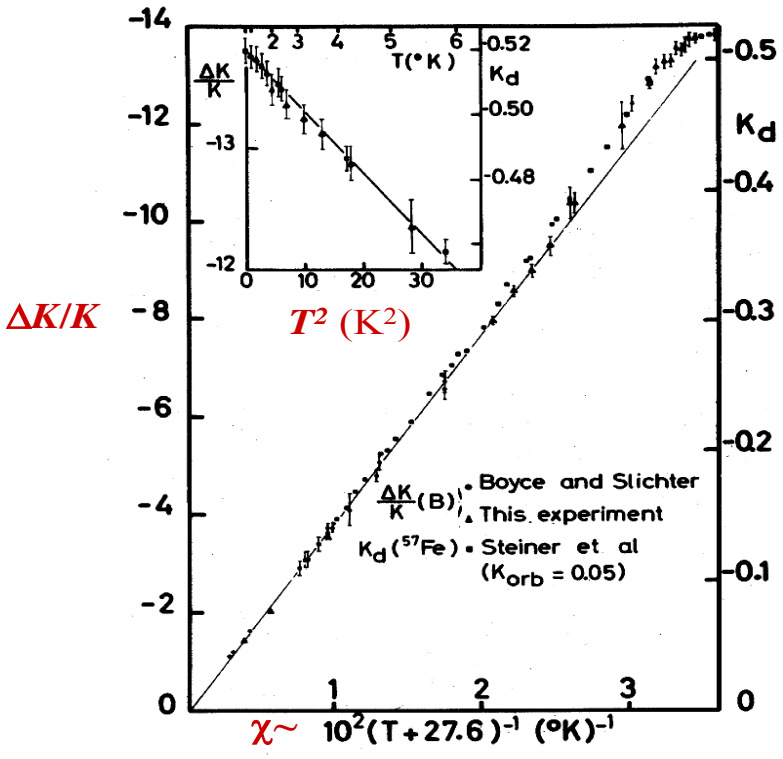

Fig. 2: *The variations of the normalized NMR shift $\Delta K/K$ induced by Fe impurities in Cu for three satellite resonances, and of the impurity susceptibility obtained by Mössbauer data (K_d) scale perfectly with each-other. This gives a good experimental determination of the variation of the local spin susceptibility through $T_K \sim 30$ K, which crosses over from a high-T Curie-Weiss dependence above T_K toward a quadratic T^2 variation below T_K (see inset) from Ref. [9].*

Cu-Cr, ~ 30 K for Cu-Fe, ~ 300 K for Au-V, etc. [8]. It was harder to consider Al-Mn along the same lines as all temperature variations were very weak in this case, so that this crossover could only occur above 1000 K, for which the alloy would have molten. Anyway, if one wanted to study experimentally the change from the magnetic state to the non-magnetic state, one needed to consider a system in which one can explore both regimes $T \gg T_K$ and $T \ll T_K$. Therefore Cu-Fe appeared immediately as the most suitable case if one wanted to avoid extremely low temperature experiments, while Cu-Mn and Al-Mn appeared as the two extreme opposite cases.

4.2 T-dependence of the susceptibility and spatial extent of the Kondo singlet

This idea of a Kondo singlet has led to some attempts to detect modifications of the host ^{63}Cu NMR width when T is decreased through T_K. Those early experiments were initially taken as a signature of the development of a static polarized cloud anti-parallel to the local impurity magnetization. But the situation was only fully clarified when NMR resonances of ^{63}Cu near neighbors to the Fe were detected (see section 3). The shifts of the various lines had T variations which scaled with each-other and displayed the same Curie-Weiss dependence as the magnetic susceptibility data taken in very dilute samples, as displayed in Fig. 2. So, on a small number

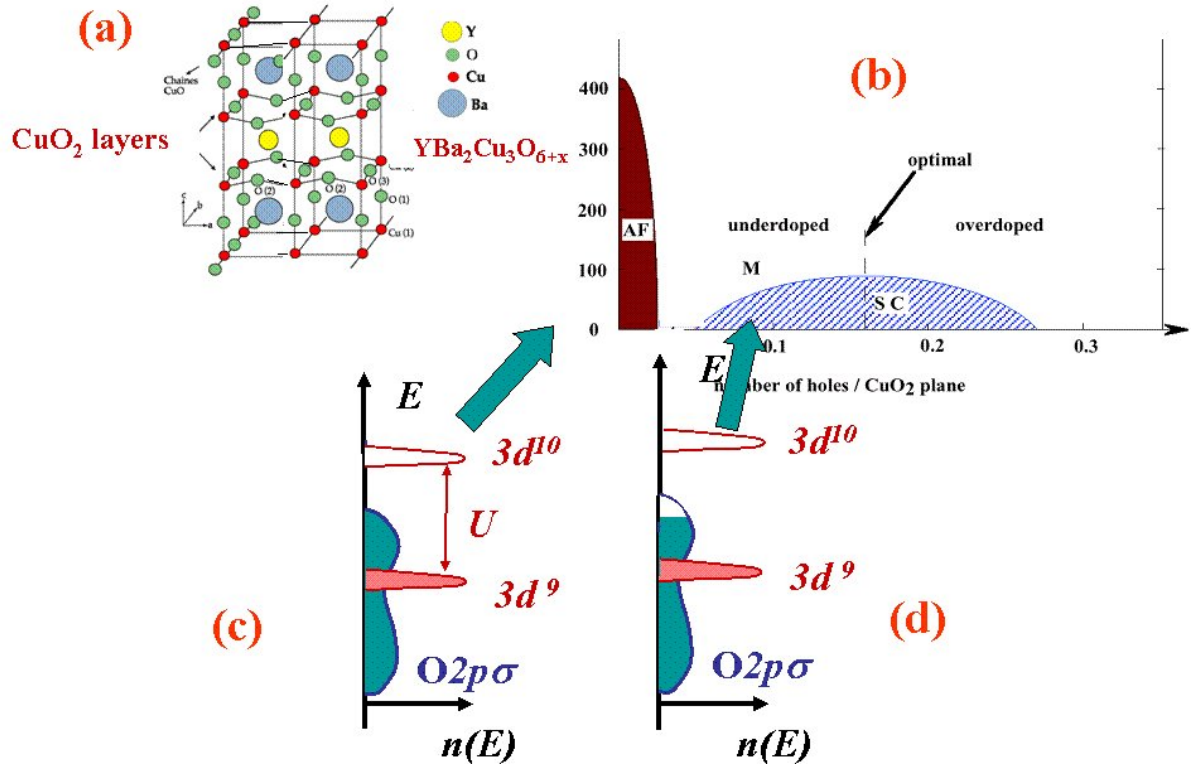

Fig. 3: **(a)** *Atomic structure of $YBa_2Cu_3O_{6+x}$. The O filling of the lower and upper CuO_x planes is responsible for hole doping.* **(b)** *Phase diagram versus hole doping of the CuO_2 planes in cuprates showing the fast decrease of the AF Néel temperature, and the SC dome.***(c)** *Band structure of the undoped parent compound.* **(d)** *possible two-band electronic structure in the absence of interaction between Cu and O holes. (Reproduced from [7])*

of sites near the impurity, the magnetic behavior does display a smooth T variation through T_K, which allowed one to deny the existence of a static compensating cloud. This result confirmed that the susceptibility reaches a low-T behavior similar to that achieved in the non-magnetic case, as has been also found by the numerical solutions of the Kondo model established by Wilson [10]. However, these results do not give any answer about the spatial extension of the correlated Kondo state (this matter is discussed in Ref. [7]).

4.3 The cuprate pseudogap

The cuprates contain as common elements CuO_2 planes (Fig. 3(a)) which are considered to contain all the important physics. Their structure is a stacking of such planes separated by other oxide layers, which maintain charge neutrality and the cohesion of the structure essentially through ionic interactions. They display the highest known superconducting temperature T_c obtained after chemical doping a parent state which is a Mott insulator. Indeed in the undoped cuprates the Cu are in a $3d^9$ state in which the Cu hole bears a $S = 1/2$ local moment (Fig. 3(c)). Those have been of course the physical properties which have driven the interest

for these systems initially both for their fundamental aspects and their potential applications. Another aspect responsible for their appeal has certainly been the fact that the carrier concentration can be easily changed by chemical heterovalent substitutions or oxygen insertion in the layers separating the CuO_2 planes, which play the important role of charge reservoirs. Electron or hole doping can then be fairly continuously controlled from zero to about 0.3 charges per unit cell, which allows one to study the evolution of the physical properties of these materials with doping and to map out their rich phase diagram (Fig. 3(b)). One important question raised concerning these doped compounds was that of the electronic structure of the band responsible for the metallic behavior. At a time when no ARPES experiments were available to map out the electronic structure, one expected that the doping holes would be located in an independent oxygen band, as exhibited in Fig. 3(d). As recalled hereafter in Sec. 4.4, the analysis of the ^{17}O,^{89}Y, and ^{63}Cu NMR shifts in $YBa_2Cu_3O_{6+x}$ cuprates has permitted to demonstrate unambiguously that the holes responsible for the measured macroscopic spin susceptibility are located on the Cu sites as expected for the undoped compound. The study of the evolution of the NMR shifts with hole doping (Sec. 4.5) allowed then to reveal the occurrence of a pseudogap in the samples with lower than optimal doping. The latter was found quite generic of the clean cuprate families (Sec. 4.6). The analysis of the NMR spin-lattice relaxation suggested a $\boldsymbol{k}$-space differentiation of the spin excitations which has been studied later in great detail by ARPES experiments (Sec. 5.3).

4.4 Carriers and hyperfine couplings

Let us assume that the Cu holes responsible for the local moments yielding the AF state of the parent compounds and the doped holes expected to be located on the oxygen orbitals are uncorrelated. In that case the macroscopic magnetic susceptibility should sum up the contributions of these two bands, while the ^{63}Cu nuclear spins would probe the spin contribution on the copper sites. Similarly the ^{89}Y and ^{17}O nuclear spins would be more likely coupled to the oxygen holes. The determination of the hyperfine fields which couple the nuclear spins with the susceptibility has been essential in the understanding of the electronic structure. The anisotropies of orbital contributions to the ^{63}Cu NMR shifts and of the ^{63}Cu spin hyperfine couplings permitted to establish that the Cu holes are located in the Cu $3d_{x^2-y^2}$ orbitals [11]. The evidence for a *negative* hyperfine coupling of ^{89}Y with the spin susceptibility allowed to demonstrate that ^{89}Y also probes the susceptibility localized on the Cu $3d_{x^2-y^2}$ orbitals through a transferred hyperfine coupling via O $2p_\sigma$ orbitals [12], which was found identical for the insulating and doped compounds. This suggested that the spin susceptibility resides in a *single spin fluid* [13], involving Cu $3d_{x^2-y^2}$ – O $2p_\sigma$ hybridized orbitals, so that the two types of holes are correlated and not independent as would be suggested by Fig. 3(d). This is fully confirmed below by the analysis of the T variations of the NMR shifts.

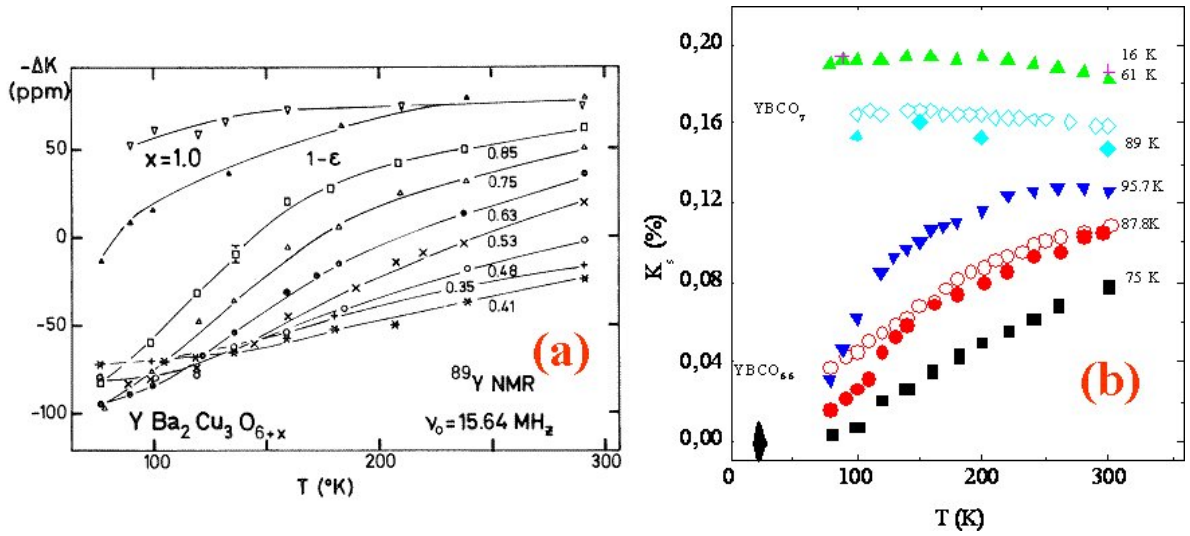

Fig. 4: **(a)** *Temperature variation of the ^{89}Y NMR shift $-\Delta K_s$ for $YBa_2Cu_3O_{6+x}$ powder samples from optimal doping to a non-superconducting sample with $x = 0.41$. The progressive increase of the pseudogap magnitude is apparent (from ref. [14]).* **(b)** *The comparison of the ^{17}O NMR-shift data in YBCO and Hg1201 permits to demonstrate that the pseudogap temperatures T^* are identical for these two compounds (from [15]).*

4.5 Evidence for a pseudogap from NMR-shift data

The optimally doped highest-T_c compounds exhibited a rather regular T-independent susceptibility together with a strange linear T variation of the resistivity above T_c. The possibility to control the hole doping in the $YBa_2Cu_3O_{6+x}$ cuprate by decreasing the oxygen content which is inserted in the intermediate planes between the CuO_2 planes permitted controlled NMR experiments in the underdoped regime for which T_c drops with decreasing hole doping. Those experiments revealed a quite distinct behavior of the NMR shifts with a dramatic drop of the spin component K_s that is of the spin susceptibility with decreasing T. Such an observation made initially by ^{89}Y NMR measurements (see Fig. 4(a)) remarkably revealed that for a composition with $T_c = 60$ K, the spin susceptibility drops by more than a factor three between room T and T_c [14]. As the spin susceptibility remains still sizable at T_c, this appeared as the signature of the opening of an imperfect gap which was qualified as a *pseudogap* already in 1989. This is remarkable inasmuch as it was not experimentally possible to detect any further sharp decrease of the spin susceptibility below T_c. The other aspect which was revealed by these experiments is that the onset-temperature T^* of the drop in K_s increases with decreasing doping. This had led to the indication that the magnitude of the pseudogap increases with decreasing doping, that is, with decreasing T_c. Most other experiments measuring uniform macroscopic responses, such as specific heat, planar resistivity ρ_{ab}, do detect an onset at similar temperatures as that of T^* [16], which is undoubtedly the highest temperature below which a detectable deviation with respect to the high-T Pauli like behavior occurs. Signatures for the pseudogap have been seen as well in optical absorption, photoemission (ARPES), or tunnel-effect experiments.

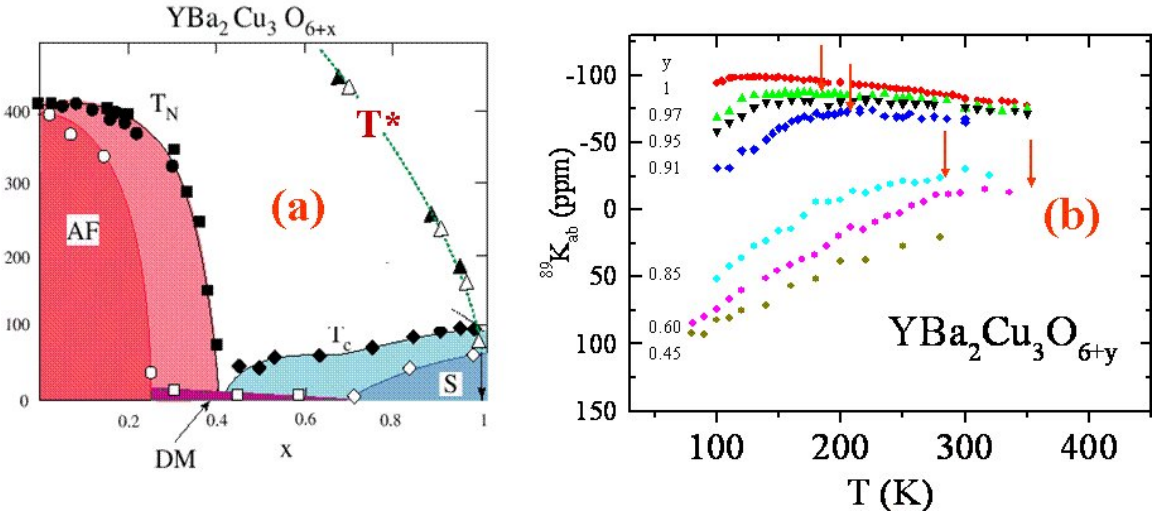

Fig. 5: **(a)** *Cuprate phase diagram obtained for $YBa_2Cu_3O_{6+x}$ by changing the oxygen content x of the Cu intermediate planes. There the phase diagram obtained for 4% Zn substitution on the Cu sites (open symbols) demonstrates that T_c is highly affected while T^* values are insensitive to disorder.* **(b)** *The determination of the T^* values from the departure of the ^{89}Y NMR shift from its high-T constant value is illustrated here by arrows. Figure composed from experimental results reported in Ref. [18].*

4.6 Universality of the pseudogap phase diagram

Data taken for the spin components of the NMR shifts for ^{63}Cu or ^{17}O in $YBa_2Cu_3O_{6+x}$ have evidenced a perfect scaling of the T variations with that of ^{89}Y, which confirmed the idea of a single spin-fluid contribution to the spin susceptibility. That was in line with the Zhang and Rice suggestion [17] that oxygen holes just form singlets with Cu and only modify the Cu susceptibility, so that the Cu and O holes are highly correlated. This identical T variation found by NMR on the various nuclear spin sites has given a universality to the pseudogap T^* deduced by NMR. Comparison between ^{17}O NMR shifts in the $YBa_2Cu_3O_{6+x}$ two-layer compound and the single layer compound $Hg_1Ba_2CuO_4$ evidenced that T^* is generic within the clean cuprate families [15] (see Fig. 4(b)). This has been confirmed by nearly all experimental determinations done by macroscopic measurements of T^*. This pseudogap T^* line introduced in the phase diagram of YBCO is displayed in Fig. 5 for pure samples but also when T_c and T_N have been decreased by 4% Zn substitution on the Cu sites, as will be discussed in Sec. 6.3.

4.7 Local magnetism induced by in-plane impurities in cuprates

An impurity is a local screened Coulomb potential, which ideally is a uniform perturbation in $\boldsymbol{q}$-space, inducing a response which is inhomogeneous in real space but which reflects the response to all $\boldsymbol{q}$ values. So quite generally, an impurity potential is a fundamental tool to probe the specific response of a pure system. For instance, the RKKY oscillations induced by a local moment impurity in a classical metal are due to the singularity associated with the truncation of the response at $|\boldsymbol{q}| = k_F$. In correlated electron systems, if some singularity occurs at a specific

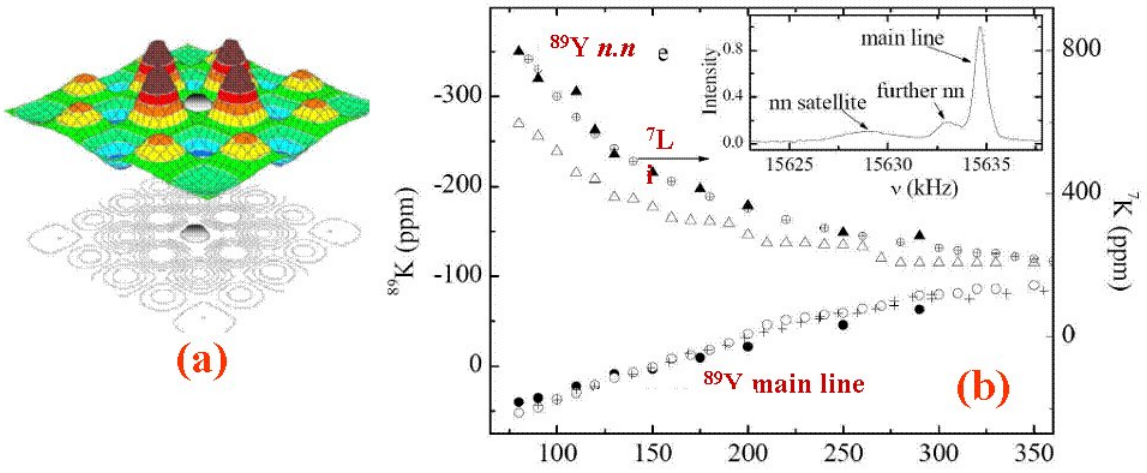

Fig. 6: **(a)** *Non magnetic impurities such as Zn or Li substituted on the Cu site in the CuO_2 plane in cuprates induce a 2D staggered magnetic response.* **(b) Inset**: *The ^{89}Y NMR spectrum exhibits a central line and satellite lines.* **Main**: *the T dependence of the satellite or ^{7}Li NMR shift permits to monitor that of the induced paramagnetism. (Figures from ref. [18]).*

"$\boldsymbol{q}$" value for a pure system, this singular response will dominate the modifications introduced by the impurity. For instance, in magnetic materials for which AF correlations can be important at a wave vector $\boldsymbol{q} = \boldsymbol{q}_{AF}$, a staggered magnetic response at this wave vector is expected. So quite generally, an impurity potential is a fundamental tool to probe the specific response of a pure system, which is all the more interesting when some physical properties might be hardly measurable directly in the pure system, or when some of the hidden physical properties can be revealed by the impurity potential. NMR experiments ideally permit to map out the spatial changes occurring around extrinsic defects. Those cannot be accessed through macroscopic non-local techniques. For instance we give evidence in Ref. [18] that the staggered magnetism induced by defects in spin chains allows to determine by NMR the correlation functions of the *pure* state. Similarly we underline hereafter that Zn or Li non-magnetic atoms substituted on the Cu sites in the cuprates induce an extended paramagnetic state in their vicinity. Such studies have been important to qualify the incidence of disorder in the various doping ranges of the cuprate phase diagram (see Ref. [18]).

As shown above, the underdoped regime of cuprates, for which a pseudogap is detected, is the interesting range, where the system is a metal with magnetic correlations, for which the use of impurities to probe the physical properties was expected to be the most fruitful. The first basic qualitative information were obtained by an approach, started in the early 1990's, using Zn and Ni impurities substituted for Cu in the $YBaCuO_{6+x}$ system specifically for $x \simeq 0.6$ for which the pseudogap occurs at $T^* \gg T_c$. The question which arose was whether a non-magnetic site induces a free paramagnetic moment in a *metallic* correlated system, as was seen later in the case of undoped spin chains and ladders. An indirect but unambiguous evidence that Zn induces a paramagnetic moment in an underdoped cuprate was obtained by monitoring the ^{89}Y NMR linewidth in $YBCO_{6.6}$:Zn_y [19]. The significant low-T increase of the linewidth that was

detected revealed the increase of the static staggered spin polarization around the impurity. This was clearly confirmed later by resolving in dilute samples the satellite NMR signals of the ^{89}Y near neighbor (*n.n.*) sites of the substituted Zn [20] (see Fig. 6(b)). This provided the first local detection of the field induced paramagnetism near the Zn, well before the equivalent information could be monitored in the case of spin chains. These data implied that the spin polarization of the Cu "n.n." to Zn is already at 100 K more than ten times larger than that of the pure host, so this was not a mere minor modification of the host density of states, but a strong effect of the electronic correlations of the system. Quite analogous ^{89}Y *n.n.* NMR data were obtained later (see Fig. 6(b)) for non magnetic Li impurities, which provided the possibility to use in the same sample the ^{7}Li, ^{89}Y, ^{17}O and ^{63}Cu nuclear spin probes. The ^{7}Li NMR permitted accurate measurements of $\chi(T)$ of the four Cu *n.n.* of the Li non-magnetic impurity. In the underdoped samples, this variation was found to display a Curie variation at low doping, which confirmed the observation made from the ^{89}Y NMR that the impurity-induced state behaves as a nearly free paramagnetic moment [21]. For increasing doping the Curie law is found to transform into a Curie-Weiss law with a Weiss temperature Θ which increases abruptly with doping. One could conclude that the low-T reduction of the susceptibility in the optimally doped case is due to the onset of the energy scale $k_B\Theta$ in analogy with the Kondo reduction of local moments in classical metallic systems. The data taken on the other nuclei has enabled the quantitative determination of the spatial structure of the induced polarization, that is, its magnitude and magnetic correlation length $\xi_{\rm imp}(T)$ which increases significantly at low T. Although $\xi_{\rm imp}$ has been found of similar magnitude at room temperature for optimal doping, it displays much weaker variations at low T than in the underdoped case. The energy scale Θ may control the T variations of both quantities, however. Since overdoping corresponds to an increase of Θ well beyond the value found for optimal doping, such a scheme would allow a smooth crossover towards the Fermi-liquid limit for large overdoping.

5 Spin-lattice relaxation

The local susceptibility measurements are giving pertinent information on the electronic properties of the material in its ground state. But NMR also permits to probe the excited electronic states through the fluctuations of the local field $\boldsymbol{B}_{\rm eff}$. This occurs through the nuclear spin-lattice relaxation (NSLR) processes which drive back the nuclear spins towards their thermodynamic equilibrium once the latter has been disturbed intentionally.

Indeed the nuclear spin magnetization is not established immediately if an external magnetic field is applied instantaneously to the material. The very interactions between the nuclear spins and the electronic degrees of freedom govern the spin-lattice relaxation time T_1 which is required to establish thermodynamic equilibrium. One typically needs transverse local field components at the Larmor frequency $h\nu_L$ to induce the difference of population of the nuclear spin levels. Therefore T_1 is directly linked with the transverse field Fourier component at ν_L of $\boldsymbol{B}_{\rm eff}(t)$. One can see that, for the hyperfine couplings considered above, this results in a measurement of the electronic dynamic susceptibility of the electron spin system.

So, in systems with unpaired spins the dominant T_1 process is due to local field fluctuations induced by the dynamics of the local electronic magnetization. Theoretically, the spin contributions to $(T_1T)^{-1}$ may be written using the imaginary part of the dynamical electron spin-susceptibility $\chi''(\mathbf{q},\nu_n)$ as

$$(T_1T)^{-1} = \frac{2\gamma_n^2 k_B}{g^2\mu_B^2} \sum_{\mathbf{q}} |A_0|^2 \, \frac{\chi''(\mathbf{q},\nu_n)}{\nu_n} \, . \tag{10}$$

Here, as for the Knight shift, we assumed that the dominant hyperfine coupling is the contact term. We shall see later many examples, which give evidence that T_1 measurements permit one to monitor the occurrence of phase transitions and to give relevant information on energy gaps between the ground state and excited states in many electronic systems. In cases where some ionic species are mobile in a material, as for instance in ionic conductors, the atomic diffusion processes can govern the local field fluctuations sensed on some nuclear spin sites, and the T_1 measurements may permit to monitor these ionic diffusion motions.

5.1 Spin-lattice relaxation in standard 3D metals

For a simple metallic band, the dynamic electronic susceptibility response is simple enough and one writes

$$\chi_0(\omega) = \sum\nolimits_{\mathbf{q}} \chi_0(\mathbf{q},\omega) = \chi_{P0} \left[1 + i\pi\hbar\omega \; \rho(E_F)\right] . \tag{11}$$

One can immediately see that this yields a simple expression for the spin-lattice relaxation from Eq. (10)

$$(T_1T)^{-1} = \pi k_B \; A_0^2 \; \rho^2(E_F)/\hbar \tag{12}$$

so that a universal relation holds between the Knight shift and T_1.

$$K^2 \, T_1T = \mathcal{S} = (\hbar/4\pi k_B) \, (g\mu_B/\hbar\gamma_{\rm n})^2 \, . \tag{13}$$

As K is T independent, this so called "Korringa" relation applies rather well in the absence of electronic correlations. As an example (see [22]) one could see that T_1T of ^{27}Al is constant in pure aluminium metal on a T range which extends over more than three orders of magnitude. The T_1 value in a metal is quite often used to define an empirical temperature scale especially in the very low T regime below 1 K.

5.2 Incidence of weak electron correlations

So far we did not consider any influence of electronic correlations though even in simple alkali metals electron-electron interactions play a role in the electronic scattering processes. We also do know that some electronic systems are on the verge of becoming magnetic. Those quasi AF or quasi ferromagnetic metals can be identified by the very fact that the Korringa relation does not apply straightforwardly as the spin susceptibility does not behave as described above for free electron Fermi liquid systems. In such cases the dynamic spin susceptibility is not uniform

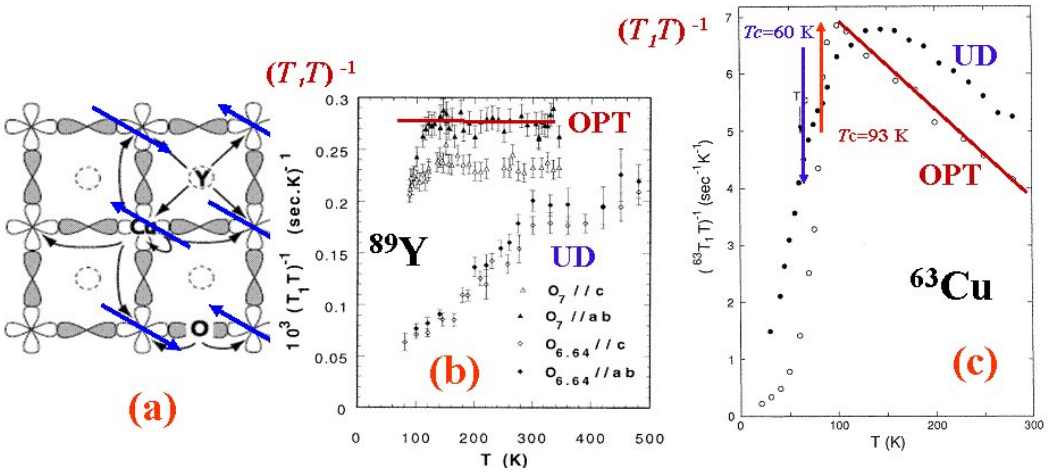

Fig. 7: **(a)** *Schematics of the Cu $3d_{x^2-y^2}$ and O $2p_\sigma$ orbitals in the CuO_2 plane showing why the AF fluctuations are filtered at the ^{17}O and ^{89}Y nuclei. This explains why the T variations of $(T_1T)^{-1}$ taken for oriented powder samples of $YBCO_7$ ($T_c = 90$ K) and $YBCO_{6.6}$ ($T_c = 60$ K) are quite different for ^{63}Cu and ^{89}Y.* **(b)** *^{89}Y data taken from Ref. [26]* **(c)** *^{63}Cu data taken from Ref. [11]. While the data for $T_c = 90$ K are T independent for ^{89}Y, as is the Knight shift, they increase at low T for ^{63}Cu. Similarly for the underdoped samples both $(T_1T)^{-1}$ and ^{89} K increase regularly up to $T^* \sim 350$ K, while those for ^{63}Cu display a maximum at $T \sim 150$ K, assigned to a spin gap.*

in q space as was shown initially by Moriya [23], and exhibits enhanced values either for $\mathrm{q} = 0$ for nearly ferromagnetic metals or for an AF wave vector $\boldsymbol{q}_{AF}$ for nearly AF materials.
In the former case the $\boldsymbol{q} = 0$ spin susceptibility is enhanced by a factor $S = 1/(1 - I\chi_{P0})$, usually called the Stoner factor, and $\chi_P = S\chi_{P0}$ exhibits a large increase with decreasing T and only saturates at very low T, as has been illustrated in the nearly ferromagnetic metals like $TiBe_2$ or in elemental Pd metal. In those cases, the enhancement of the dynamic spin susceptibility $\chi_0(\boldsymbol{q}, \omega)$ is not uniform in $\boldsymbol{q}$ space and is weaker for $\boldsymbol{q} \neq 0$, therefore the Knight shift is more enhanced than $(T_1T)^{-1}$. The Korringa relation does only apply when χ_P saturates [24], with a $T = 0$ Korringa constant $K^2T_1T = \mathit{\Delta}\,\mathcal{S}$ increased by an S-dependent factor $\mathit{\Delta}(S)$. On the contrary in nearly AF metals $\chi_0(\boldsymbol{q}, \omega)$ is peaked for $\boldsymbol{q} = \boldsymbol{q}_{AF}$ which means that the static spin susceptibility and the Knight shift K are less enhanced than $\chi_0(\boldsymbol{q}_{AF}, \omega)$. Correspondingly $K^2T_1T = \mathit{\Delta}\,\mathcal{S}$ corresponds in that case to $\mathit{\Delta} < 1$, that is a decreased Korringa constant, as has been seen for instance in the compound MnSi [25].

5.3 Dynamic spin susceptibility and electronic correlations

We shall discuss below the actual information on the AF correlations given by the measurements of the spin-lattice T_1 and transverse T_2 nuclear spin relaxation in the cuprates. As shown in the previous section, the T_1 give determinations of $\chi''(\boldsymbol{q}, \omega)$ while we shall show here that the transverse T_2 is related to $\chi'(\boldsymbol{q}, 0)$.
The feature which had been clearly evidenced was that for ^{89}Y nuclear spins $(T_1T)^{-1}$ and ^{89}K have very similar T variations (with T and doping). This is illustrated in Fig. 7(b) on data

taken on field-aligned YBCO samples realized for two compositions, O_7 for which $(T_1T)^{-1}$ is T independent as is ^{89}K, while for $O_{6.6}$ both quantities exhibit large T increases. Similar results on the ^{17}O NMR have been obtained, which established that the dynamic susceptibility viewed by these nuclei appeared quite correlated with the static susceptibility. It has been established that T_1TK_s is nearly T independent, which has been taken as an evidence for the presence of a Fermi-liquid like component in the magnetic response.

However, as was seen by many authors, the $(T_1T)^{-1}$ of ^{63}Cu behaves quite differently (for references, see Ref. [27]). In the optimally doped compound $(T_1T)^{-1}$ increases at low T while it goes through a maximum at a temperature much lower than T^* in the underdoped sample (see Fig. 7(c)). This difference between ^{63}Cu and ^{17}O (or ^{89}Y) NMR is understood as the two latter nuclear spins being coupled to two (or four) Cu moments do not detect AF fluctuations at the AF wave vector $\boldsymbol{q}_{AF} = (\pi, \pi)$, as sketched in Fig. 7(a). In other words, the ^{63}Cu data uniquely reveals the occurrence of a peaked response of $\chi''(\boldsymbol{q}, \omega)$ at $\boldsymbol{q}_{AF}$. This has been confirmed directly by inelastic neutron scattering experiments taken on underdoped samples. The maximum in $(T_1T)^{-1}$ for ^{63}Cu has been assigned to a spin gap which is quite distinct from the pseudogap T^*. It would increase much less rapidly than T^* for decreasing doping. Both the pseudogap T^* and the spin gap are detected only in underdoped samples, which suggests that they are connected.

Let us point out now that this strong magnetic response in cuprates induces a contribution to the nuclear spin transverse T_2 relaxation, which has been found to be quite important on the Cu sites. In weakly correlated solids T_2, which is measured with spin-echo experiments (see NMR wikipedia) is usually fully determined by the direct dipole-dipole interactions between nuclear spins. In cuprates and more generally in correlated systems, a nuclear spin at $\boldsymbol{R}_i$ can be viewed as a moment which induces, through the $\boldsymbol{q}$-dependent susceptibility $\chi'(\boldsymbol{q}, 0)$, a polarization of the electronic spins which extends on the sites nearby $\boldsymbol{R}_i$. This polarization does in turn couple to the nuclear spins on these sites. This indirect (RKKY-like) dipolar interaction between the nuclear spins induces a contribution to the spin echo decay. After summation of the interaction of a nuclear spin with all its neighbors, the spin echo is found to get a Gaussian decay with a time constant T_{2g} given by

$$\left(1/T_{2g}\right)^2 \propto A_{\mathbf{0}}^4 \sum_{\boldsymbol{q}} [\chi'(\boldsymbol{q}, 0)]^2 - A_{\mathbf{0}}^4 \left[\sum_{\boldsymbol{q}} \chi'(\boldsymbol{q}, 0)\right]^2 .$$

In the cuprates, $\chi'(\boldsymbol{q}, 0)$ is expected to be peaked at $\boldsymbol{q}_{AF}$ and the width of the peak defines a correlation length ξ for the AF response, which might be estimated from the T_{2g} data. Even in the underdoped pseudogapped regime ξ is found to increase steadily with decreasing T as has been seen as well from impurity studies described in Sec. 4.7.

Coming back to the pseudogap, more recently ARPES or STM experiments have given evidence that a gap in the charge excitations only occurs for the antinodal directions $(0, \pi)$ in $\boldsymbol{k}$-space. So the closed Fermi surface which occurs at high T in underdoped cuprates loses weight in the antinodal directions when T decreases, and the Fermi surface then reduces to Fermi arcs, which shrink with decreasing T (see [28]). The experimental results on $(T_1T)^{-1}$ of

^{63}Cu are certainly precursor indications of this $\boldsymbol{k}$-space differentiation which has been found by $\boldsymbol{k}$-dependent spectroscopies.

Phenomenological attempts have been done to describe the shape functions of the spin susceptibilities $\chi''(\boldsymbol{q},\omega)$ and $\chi'(\boldsymbol{q},0)$, in order to fit the NMR data [29]. Satisfactory qualitative descriptions could be achieved, with ξ values of about two lattice constants at room T in both the optimal and underdoped samples, with much larger low-T increases of ξ in the latter. However, these approaches required to introduce by hand the Fermi liquid like metallic component and did not include explicitly the occurrence of the pseudogap. A complete theory of the physical phenomena at play would require a model which generates altogether the pseudogap, the AF correlation length and its T variation.

To conclude, the pseudogap is most probably intimately linked with the correlated nature of these systems, and its actual physical origin is intensely debated. One interpretation, proposed quite early on, is that it represents a precursor pairing state, the superconducting phase being only established at T_c when the pairs achieve long-range phase-coherence [30]. Such an interpretation would imply that the SC gap increases with decreasing T_c. This is so far contradicted by direct or indirect determinations of the SC gap. Another class of interpretations could be the establishment of a hidden order disconnected from superconductivity, such as a spin ordering, for instance a Resonant Valence Bond (RVB) state (see [31]), a d density wave (ddW), a charge segregation into stripe order or an ordering involving orbital currents. Such possibilities have been recently underlined by experimental discoveries of such type of orders, which appear system dependent, and often occur at temperatures below T^*. These experiments are so novel that they have initiated vivid debates on the pseudogap, but did not permit so far to resolve the issues they raised. The pseudogap remains still today the central point debated on the cuprates and at the present writing the understanding of the pseudogap state remains controversial. The author believes that magnetic short-range correlations explain the pseudogap crossover at T^* and the Fermi surface differentiation, while the orders detected at lower T than T^* are rather consequences of the pseudogap formation than direct manifestations of the pseudogap itself.

6 NMR in superconductors

Obviously, the establishment of a SC state yields profound transformations of the electronic properties which will be seen in the NMR response. NMR experiments do not only evidence the occurrence of SC. They also permit to characterize the properties of the SC electronic state [32].

6.1 Knight shift, relaxation, and gap in the SC state

One of the major effects which occur for phonon mediated SC in usual metals is the pairing of electrons in a singlet state. Such a pairing suppresses totally the normal state spin susceptibility at $T = 0$. This is seen quite simply as a full suppression of the spin contribution K_s to the Knight shift in NMR. In type I superconductors, the magnetic induction vanishes in the Meiss-

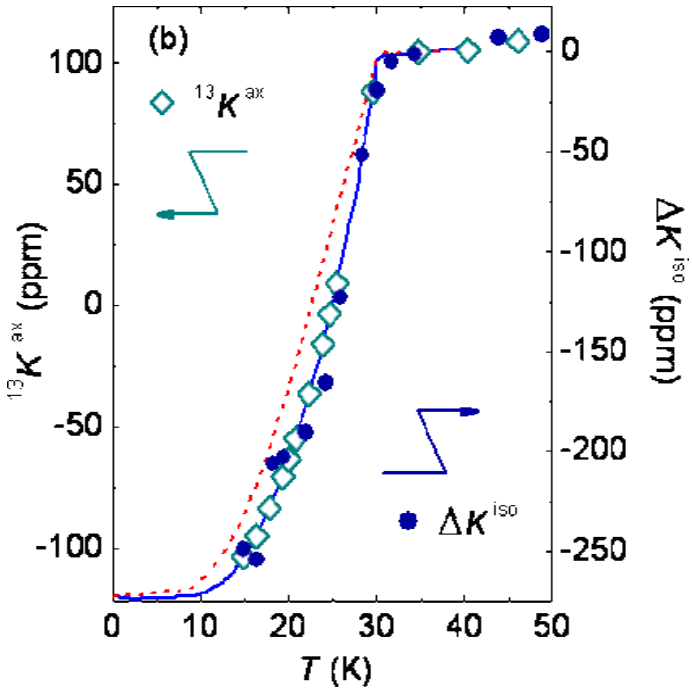

Fig. 8: *The ^{155}Cs and ^{13}C NMR shifts measured in the Cs_3C_{60} phase are plotted versus T below the superconducting temperature $T_c = 30$ K. The NMR shifts follow the standard Yosida type decrease expected for singlet superconductivity [33].*

ner state which by itself forbids observation of the NMR signal in the SC state. But in type II superconductors the field penetrates as an array of vortices, which becomes so dense near the upper critical field H_{c2} that it becomes possible to detect the NMR signal in that regime, and to see the suppression of the Knight shift. Taking into account the variation of the SC gap and the thermal population at temperatures near T_c, yields a specific T dependence of the spin susceptibility, that is of $K_s(T)$, which has been computed by Yosida [6], and which is given by

$$K_s(T)/K_n = \int_{\Delta}^{\infty} \frac{N(0)|E|}{\sqrt{E^2 - \Delta^2}} \frac{df}{dE} dE \,. \tag{14}$$

Here f is the Fermi function. The actual variation of the Knight shift with decreasing temperature can be measured and displays an agreement with this Yosida function as can be seen in Fig. 8 in the particular case of Cs_3C_{60}. As for spin-lattice relaxation data, it can be taken in type I SC using ingenious tricks such as experiments in which the external field is cycled from a field exceeding the critical field H_c down to a field $H < H_c$ in which the nuclear spin magnetization is let free to evolve under the influence of the electronic system.

The opening of the SC gap yields an activated exponential increase of the NMR spin-lattice relaxation rate as T approaches 0, which permits a determination of the SC gap magnitude from the corresponding low T variation of T_1^{-1} (Fig. 9). However the great advance of BCS theory has been its ability to describe the excited states in the SC state up to T_c. Indeed in such a BCS SC state subtle effects are revealed by T_1T data taken near T_c. An increase of the spin-lattice relaxation rate above the normal state Korringa value takes place below T_c. This

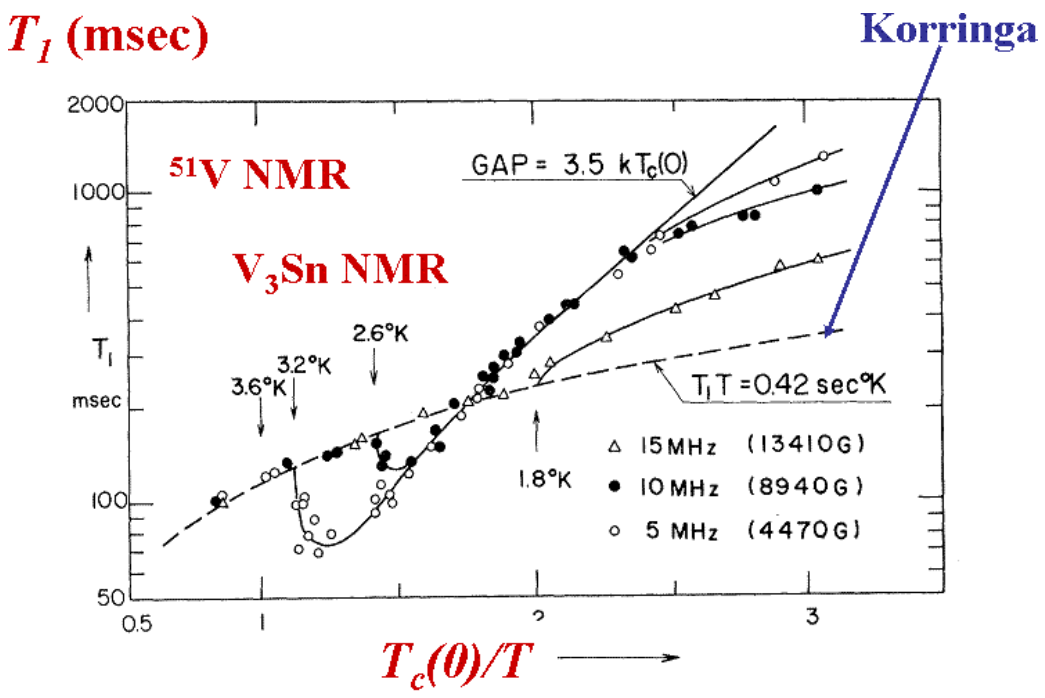

Fig. 9: *The $\log(1/T_1)$ of ^{51}V in V_3Sn is plotted versus $1/T$ for three distinct applied fields, which induce changes of T_c. In the normal state above T_c the relaxation rate is field independent with T_1T=0.42 sec°K. Below T_c the reduction of T_1 represents the Hebel Slichter coherence peak. At low T all curves point towards an activated behavior associated with the full opening of the superconducting gap (adapted from Ref. [32]).*

so called coherence peak evidenced by Hebel and Slichter [34] results partly from the thermal population of the increased density of electronic states which piles up above the SC gap. The T_1 only lengthens at somewhat lower temperatures than T_c (see Fig. 9).
Both these discoveries of the decrease of the spin susceptibility and of the occurrence of a Hebel-Slichter coherence peak have given the early evidences for the applicability of BCS theory of superconductivity in usual metallic systems.

6.2 Field distribution in the mixed state of type II superconductors

In type II superconductors the magnetic induction varies significantly in space in the mixed state. This leads to a distribution of Larmor frequencies for the nuclear spins in the material. The shape of the NMR spectrum reconstitutes the histogram of the magnetic fields. Close to H_{c2}, singularities appear in the spectrum for values of the magnetic field corresponding to the extrema of the field distribution. The shape and width of the observed resonance can be used to deduce λ, the magnetic field penetration depth. However, for experimental reasons, NMR is not the best method for studying the superconducting state. A related technique uses elementary particles called muons. These behave like heavy electrons (or light protons), and have the property of decaying by emission of positrons in the direction of their spin. A muon whose spin is initially polarized perpendicularly to the field B_0 is implanted in the sample at

time zero. One then observes the direction of the emitted positrons when it decays. By repeating this experiment for a large number of events, the free precession signal of the muon spin can be reconstructed statistically. This experiment is equivalent to an NMR experiment, and can be used to determine λ. Since muons can be implanted in almost any sample, it has been possible to make comparative measurements of λ in a wide range of superconducting materials.

6.3 Exotic superconductivities

The importance of the cuprates in the physics of correlated systems has resulted from the discovery that, when the AF is suppressed by hole doping, the doped metallic state which results has a SC ground state and displays strange metallic and magnetic properties. The most surprising feature has been the fact that the superconductivity discovered in these materials has the highest critical temperatures T_c found so far in any superconducting material, and exceeds any T_c which could be expected within the BCS approach known to apply in classical metallic states. An important observation in the cuprates has been the fact that the phase diagram with increasing hole doping displays a dome-shaped SC regime, that is, SC disappears for dopings beyond about 0.3. These non-expected features have immediately led to the idea that SC in the cuprates has an exotic origin linked with electron-electron interactions rather than the classical electron-phonon driven superconductivity which prevails in classical metals.

Obviously, the establishment of any SC state yields profound transformations of the electronic properties which are reflected in the NMR response. In BCS Superconductors the formation of singlet Cooper pairs is directly seen as a loss of the normal state spin susceptibility, that is, a drop of the NMR shift, as evidenced hereabove. NMR studies appeared then quite important in the early days after the discovery of HTSC. One indeed was interested to see whether BCS like observations would be made. For HTSC samples with high T_c around the optimal doping, the NMR data appear quite similar to those obtained in standard BCS materials inasmuch as the NMR shift of most nuclear species in the material ^{63}Cu, ^{17}O, ^{89}Y were found T independent down to T_c, and dropped abruptly at T_c in accord with spin-singlet superconductivity Fig. 10(a) [35]. In many cases for which SC is probably also more exotic than for phonon mediated SC the pairing state remains a singlet, which has been confirmed by similar NMR-shift studies.

In some exotic SC states the pair wave function can be in a spin-triplet state, a situation which has been found first for superfluidity of ^{3}He which are fermions which bind to form spin-triplet Cooper pairs [36]. As a spin triplet can be in three distinct states either $|\uparrow\uparrow\rangle, |\downarrow\downarrow\rangle, |\uparrow\downarrow\rangle + |\downarrow\uparrow\rangle$ or quantum superpositions of these components, the magnetic response to an applied field depends on the actual state of the bound pairs. This explains why ^{3}He has two different triplet superfluid phases. Phase A with equal spin states formed by $|\uparrow\uparrow\rangle$ and $|\downarrow\downarrow\rangle$ pairs displays no change of the nuclear spin susceptibility though the superfluid transition, while phase B is an equal superposition of the three states which leads to a marked decrease of the spin susceptibility which, however, does not vanish completely at $T = 0$.

In correlated electron systems one similarly expects that with spin-triplet SC the behavior of the NMR shift below T_c should permit to establish the spin-triplet pairing and to determine the

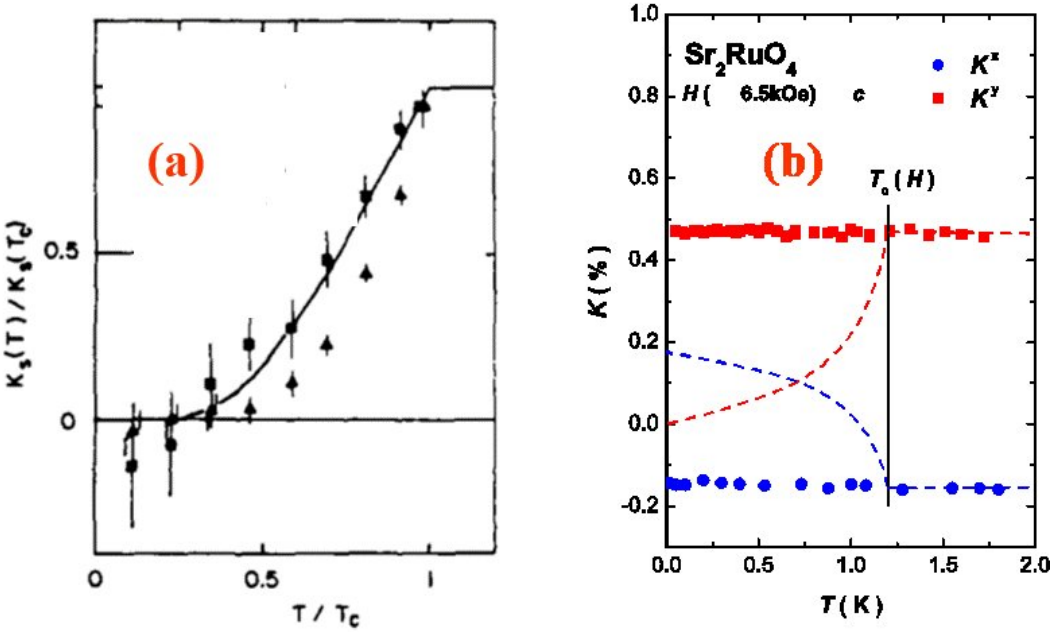

Fig. 10: *^{17}O NMR-shift data taken below T_c in the two planar directions* **(a)** *in $YBaCuO_7$ it drops below T_c and vanishes for $T \ll T_c$ [35].* **(b)** *in Sr_2RuO_4 it remains constant through T_c, which supports spin-triplet superconductivity. Here the reported lines would correspond to expectations for a singlet SC case (from ref. [37]).*

superposition of spin states. A system which has been thoroughly studied is Sr_2RuO_4, in which the RuO_2 form a square lattice which is similar to that of the cuprate La_2CuO_4. Indeed it has been shown in that compound that both ^{17}O and ^{99}Ru NMR shifts exhibit absolutely no change though T_c, Fig. 10(b), which is a strong case for spin-triplet SC with equal spin states [37]. Once the spin properties of the pairs has been established, their orbital state has a symmetry which is imposed by the total antisymmetry of the wave function. So that an antisymmetric spin-singlet state implies an even orbital state, that is an s- or d-wave symmetry of the wave function. Similarly for a symmetric triplet state, the orbital wave function should be antisymmetric that is p-wave or higher order. In most of these exotic pairing states the SC gap is not uniform over the Fermi surface as is the case for most phonon mediated cases. In these exotic superconductors the gap depends of the wave vector $(\boldsymbol{k}, -\boldsymbol{k})$ of the pairs and might exhibit gap nodes for some $\boldsymbol{k}$ values or some wave vector directions. For instance for a 2D system, if the gap has a d-wave order-parameter symmetry, the gap changes sign and therefore vanishes along two axes of the unit cell. This implies that the gapless states will be filled much faster with increasing T than in a pure s-wave BCS superconductor.

In such spin singlet states the functional form of the increase of the spin susceptibility (that is of the NMR shift) with increasing temperature from $T = 0$ permits, in principle, to determine whether nodes occur in the gap function. Experimentally this is somewhat difficult to establish from NMR shift measurements which have limited accuracy at low T due to the inhomogeneous field penetration in the vortex lattice. This is however much more accessible from $1/T_1$ data

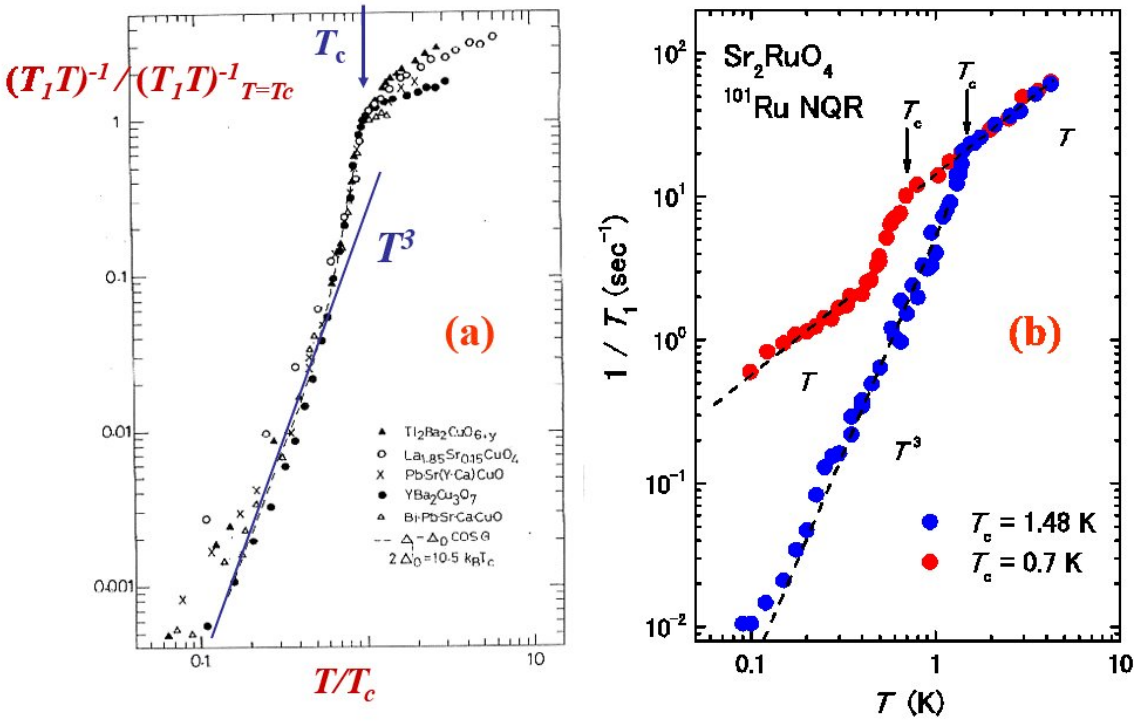

Fig. 11: **(a)** *In $YBaCuO_7$ the ^{63}Cu $1/T_1$ data has a T^3 dependence, which agrees with d-wave SC [38].* **(b)** *In Sr_2RuO_4 the sample-dependence of the Ru NQR $1/T_1$ data is illustrated. The use of a clean sample permits to evidence a T^3 variation which establishes the existence of nodes in the gap function [39].*

which display then a power law increase with an exponent that depends of the wave vector dependence of the gap. A T^3 variation of $1/T_1$ has been best evidenced by zero-field NQR experiments in cuprates, which is in accord with the d-symmetry of the SC order-parameter, Fig. 11(a) and [38]. Though these NMR data were rather conclusive, this d-wave symmetry has such an implication for the understanding of the pairing mechanism that it has only been fully accepted within the community when ARPES and phase-sensitive tunneling experiments established it independently. One has however to recall that low-T NMR measurements can be contaminated by extra contributions of impurities to the relaxation. So to conclude about the symmetry of the SC order-parameter in a given compound, great care has to be taken to avoid the presence of impurities in the actual materials. This is for instance illustrated in Fig. 11(b) for the spin-triplet SC of Sr_2RuO_4, for which a T^3 variation of $1/T_1$ has also been found once clean samples could be produced [39]. Here again this result points out the existence of lines of gap nodes, though their spatial location on the Fermi surface is not yet clarified. The spatial structure of the p-wave state symmetry which governs SC in this compound is therefore not yet fully characterized. A p-wave spin-triplet state has been proposed as well from NMR experiments in some Heavy Fermion compounds such as UPt_3 or in low-dimensional organic conductors, although more experimental confirmations would be required to fully establish the validity of these proposals.

7 Summary

Most, if not all, the discoveries which have been done since the 1980's on correlated-electron systems resulted from extensive experimental investigations. In this lecture I have shown that the NMR technique has been quite successful in this process. This has been exemplified here by revealing some important problems highly debated nowadays in correlated-electron physics. The main impact of NMR comes about as preliminary experiments can be done on powder materials which are not perfect. The second aspect which highlights this technique is that NMR results, which are not surface sensitive, are quite reproducible so that most results presented here have usually been confirmed by independent investigations done in different laboratories on distinct sample materials. All this is eased by the fact that NMR experiments allow one to detect the incidence of defects and disorder effects on the very samples on which the data are taken. We have shown here that the introduction of specific defects, associated with the capability to detect locally their incidence is a powerful tool to unravel the properties of the pure material. This altogether has induced large efforts to clarify the incidence of disorder on the properties of correlated-electron systems. A similar advantage has been highlighted as well for the STM techniques, which however require samples with sufficient surface quality and do not probe the magnetism induced by defects.

As emphasized in many instances in this article, NMR permits to probe on the local scale a large set of relevant physical quantities ranging from magnetic susceptibility, the spin fluctuations, the superconducting properties etc.. In metallic correlated electron systems, an important aspect is the ability to identify by NMR the electronic band(s) which are involved in the metallic state and to establish whether magnetism is associated with different degrees of freedom or due to the same bands. Coming to SC, one of the points which has attracted most attention is its interference (destructive or constructive) with metallic magnetism. The cuprates are in that respect certainly exotic superconductors, in which the incidence of electron correlations and AF short range interactions can be essential to drive superconductivity, or at least enhance the SC transition temperatures. Many other materials have been shown to display situations where magnetism and SC are proximate to each-other in phase diagrams. In Fe superconductors (pnictides or chalcogenides) the phase diagrams are sometimes spanned by doping as in the cuprates, but in other families of compounds the phase diagrams are spanned by pressure control of the overlap integrals as for organic, heavy fermions, or Cs_3C_{60} compounds.

In most of these cases a thorough experimental characterization of the SC order-parameter symmetry is needed prior to any determination of the pairing glue, and NMR data can be helpful in that respect. The d-wave symmetry of the order-parameter for cuprates is considered as the strongest indication that electronic correlations could be responsible for the pairing in these compounds. Even for materials less correlated than the cuprates the incidence of electronic correlations is definitely less detrimental to SC than initially expected and the existence of AF correlations in the material could as well be the boson field mediating the SC state. Many possible glues between electrons such as phonons, AF fluctuations, or charge correlations near a Quantum Critical Point, have been considered and may be at work in distinct materials. But all

this is far from being settled and requires thorough investigations specific to the various families of correlated-electron materials.

We did address here only a limited number of correlated-electron families of compounds which have been investigated using NMR techniques. One might find in Ref. [4] many other striking examples, such as 1D organic compounds, nanotubes, heavy fermions, Na cobaltates, or Kagome compounds with magnetic frustration leading to spin-liquid ground states, on which successful NMR experiments have been undertaken. Other examples are compounds on which NMR techniques permitted to study recently the insulator to metal transition induced by pressure in undoped half-filled systems, that is the actual Mott transition. This has been made possible by the recent discovery of quasi 2D organic and 3D alkali fulleride compounds, which display quasi ideal 2D or 3D Mott transitions.

Finally I should mention at this stage that I did not address here one important aspect of the NMR technique which takes advantage of nuclear quadrupole effects detected in NMR for nuclear spins with $I > 1/2$. Those quadrupole splittings of the NMR spectra usually permit to distinguish the charge environment of these nuclei. In correlated electronic solids this gives an access to charge differentiation on atomic sites or to charge density waves due to Fermi surface reconstruction when they do occur. This is also illustrated in Ref. [4] in the case of layered Na cobaltates or for the CDW which occurs well below the pseudogap T^* in underdoped cuprates [40]. The latter experiments have triggered new ideas about the origin of the pseudogap in the cuprates, but while the pseudogap T^* is generic, the CDW order and its symmetry appear somewhat dependent of the cuprate family. Therefore the charge order appears as a consequence of the pseudogap rather than its actual origin. An important tendency towards charge ordering situations has been proposed to dominate the ground state properties of correlated electron systems. Quadrupolar effects in NMR ideally permit to unravel such situations in great detail.

I shall conclude here that the description of some selected experimental cases given in this lecture permitted us to underline the importance of the NMR technique and to reveal altogether to the reader a wide range of novel phenomena specific to correlated-electron physics.

References

[1] H. Alloul: *Introduction to the physics of Electrons in Solids* (Graduate Texts in Physics, Springer, Heidelberg, 2011)

[2] A. Abragam: *The Principles of nuclear magnetism* (Clarendon Press, London, 1961)

[3] C.P. Slichter, *Principles of Magnetic Resonance* (Harper and Row, 1963 and Springer-Verlag, New York, 1989 (3rd ed.))

[4] H. Alloul: *NMR in strongly correlated materials*, Scholarpedia, 10(1):30632 (2015)

[5] W.D. Knight: *Magnetic Resonance and relaxation*, in Ed. R. Blinc, North Holland 311 (1967)

[6] K. Yosida, Phys. Rev. **110**, 769 (1956)

[7] H. Alloul, J. Supercond. Nov. Mag. **25**, 385 (2012)

[8] M.D. Daybell and W.A. Steyert, Rev. Mod. Phys. **40**, 380 (1968)

[9] H. Alloul, Phys. Rev. Lett. **35**, 460 (1975)

[10] K.G. Wilson, Rev. Mod. Phys. **47**, 773 (1975)

[11] M. Takigawa, A.P. Reyes, P.C. Hammel, J.D. Thompson, R.H. Heffner, Z. Fisk, and K.C. Ott, Phys. Rev. B **43**, 247 (1991)

[12] H. Alloul, P. Mendels, G. Collin and P. Monod, Phys. Rev. Lett. **61**, 746 (1988)

[13] F. Mila and M. Rice, Physica C **157**, 561 (1989)

[14] H. Alloul, T. Ohno and P. Mendels, Phys. Rev. Lett. **63**, 1700 (1989)

[15] J. Bobroff, H. Alloul, P. Mendels, V. Viallet, J.F. Marucco, and D. Colson, Phys. Rev. Lett. **78**, 3757 (1997)

[16] T. Timusk, and B. Statt, Rep. Prog. Phys. **62**, 61 (1999)

[17] F.C. Zhang and T.M. Rice, Phys. Rev. B **37**, 3759 (1988)

[18] H. Alloul, J. Bobroff, M. Gabay and P. Hirschfeld, Rev. Mod. Phys. **81**, 45 (2009)

[19] H. Alloul, P. Mendels, H. Casalta H., J.F. Marucco and J. Arabski, Phys. Rev. Lett. **67**, 3140 (1991)

[20] A.V. Mahajan, H. Alloul, G. Collin, and J.F. Marucco, Phys. Rev. Lett. **72**, 3100 (1994)

[21] J. Bobroff, A. Mac Farlane, H. Alloul, P. Mendels, N. Blanchard, G. Collin, and J.F. Marucco Phys. Rev. Lett. **83**, 4381 (1999)

[22] H. Alloul, *NMR studies of electronic properties of solids*, Scholarpedia, 9(9):32069 (2014)

[23] T. Moriya, Prog. Theor. Phys. **16**, 23 (1956)

[24] H. Alloul and L. Mihaly, Phys. Rev. Lett. **48**, 1420 (1982)

[25] M. Corti, F. Carbone, M. Filibian, Th. Jarlborg, A.A. Nugroho, and P. Carretta, Phys. Rev. B **75**, 115111 (2007)

[26] H. Alloul, A. Mahajan, H. Casalta and O. Klein, Phys. Rev. Lett. **70**, 1171 (1993)

[27] R.E. Walstedt: *The NMR probe of High Tc materials* Springer Tracts in Modern Physics, Vol. 228 (2008)

[28] A. Kaminski, T. Kondo, T. Takeuchi, and G. Gu, Phil. Mag., (2014)

[29] A.J. Millis, H. Monien, and D. Pines, Phys. Rev. B **42**, 167 (1990)

[30] V.J. Emery and S.A. Kivelson, Nature **374**, 434 (1995)

[31] P.W. Anderson, Science **235**, 1196–1198 (1987)

[32] D.E. Mac Laughlin: *Magnetic Resonance in the Superconducting state* Solid State Physics **31**, 1 (1976)

[33] P. Wzietek, T. Mito, H. Alloul, D. Pontiroli, M. Aramini and M. Riccò, Phys. Rev. Lett. **112**, 066401 (2014)

[34] L.C. Hebel and C.P. Slichter, Phys. Rev. **113**, 1504 (1957)

[35] M. Takigawa, P.C. Hammel, R.H. Heffner, Z. Fisk, K.C. Ott, and J.D. Thompson, Physica C **162-164**, 853 (1989)

[36] A.J. Leggett, Rev. Mod. Phys. **47**, 331 (1975)

[37] K. Ishida, H. Mukuda, Y. Kitaoka, K. Asayama, Z.Q. Mao, Y. Mori, and Y. Maeno, Nature **396**, 658 (1998)

[38] K. Asayama, G.-Q. Zheng, Y. Kitaoka, K. Ishida, and K. Fujiwara, Physica C **178**, 281 (1991)

[39] K. Ishida, H. Mukuda, Y. Kitaoka, Z.Q. Mao, Y. Mori, and Y. Maeno, Phys. Rev. Lett. **84**, 5387 (2000)

[40] T. Wu, H. Mayaffre, S. Kramer, M. Horvatic, C. Berthier, W.N. Hardy, R. Liang, D.A. Bonn, and M.-H. Julien, Nature **477**, 191 (2011)